

Structural and topologic aspects of carbonium ions (C=1-4)

Nora B. Okulik¹, Alicia H. Jubert², and Eduardo A. Castro^{3,*}

¹Universidad Nacional del Chaco Austral, Cte. Fernández 755, (3700) P. R. Sáenz Peña, Chaco, ²Programa CEQUINOR, Departamento de Química, Facultad de Ciencias Exactas y Facultad de Ingeniería, UNLP, Calle 47 y 115, La Plata 1900, Buenos Aires, ³INIFTA, División Química Teórica, Departamento de Química, Facultad de Ciencias Exactas, UNLP, Diag. 113 y 64, Suc. 4, C.C. 16, La Plata 1900, Buenos Aires, Argentina

ABSTRACT

Since the original Olah's discovery a large number of carbocations have been prepared and their properties studied in great detail. Stable carbocations could be prepared through the use of extremely acidic compounds. Thus, pentacoordinated carbonium ions have been obtained from methane higher alkanes and various cycloalkanes. However, the characterization of these protonated species using spectroscopic techniques is a difficult task to accomplish. This fact reveals the importance of using theoretical tools to complement experimental efforts to study suitably these chemical ions. In this review, we present an exhaustive study on structural investigations and topologic characterizations using atoms-in-molecules method of carbonium ions (C=1-4) in order to get a suitable improvement of our understanding of the chemical bonding in these species.

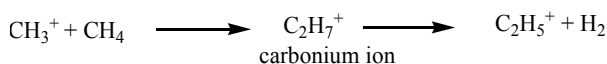
KEYWORDS: carbocations, three-centre bonds, C₁-C₄ alkanes, activation

INTRODUCTION

In the 1920s and 1930s, when some chemists started detailed studies of how chemical reactions between organic molecules took place, it became apparent that positively charged hydrocarbons

(named "carbocations") actually could occur as very short lived intermediates in the chemical reactions. It was generally assumed that one would never be able to prepare them in some quantities, but the direction of this field changed completely through the original and imaginative work of George A. Olah and co-workers in the early 1960s. They discovered that stable carbocations could be prepared through the use of a new type of extremely acidic compounds, far stronger than well known inorganic acids like sulphuric acid, hydrochloric acid, etc. These new acids became generally known as superacids, and they are so strong that they can protonate such extremely weak bases as the alkanes.

Five and higher coordinated carbocations, obtained from methane higher alkanes and various cycloalkanes, play an increasingly important role in the preparation and transformation of hydrocarbons. Besides the interest of simple reactions between alkanes with protons in gas phase (mostly by mass spectrophotometry) and the condensed phase (in superacid media) there is also considerable interest in the transformation of lower carbocations, such as the methyl cation, in higher cations. For example, the reaction with the methyl cation and methane:



This process is continued by producing protonated higher hydrocarbons. In fact, this is a process of

*Corresponding author
castro@quimica.unlp.edu.ar

the transformation of methane into the highly desirable hydrocarbons [1].

The role of five coordinate carbocations is also of substantial importance in other hydrocarbon transformations, such as isomerizations of alkanes, as well as electrophilic reactions of *n*-donor hydrocarbons (olefins, aromatics) [2].

Carbocations

Carbocations are cations containing an even number of electrons in which the positive charge is formally located at one or more carbon atoms. For many years R_3C^+ species were called “carbonium ions”, although it was suggested [3] that this was inappropriate because “-onium” usually refers to a covalency higher than that of the neutral atom. Nevertheless, the name “carbonium ions” was well established and gave rise to some few problems until some years ago, when George Olah and his co-workers found evidence for another type of intermediate in which there is a positive charge at a carbon atom, but in which the carbon atom bears a formal covalence of five rather than three [4]. Olah proposed [5] that the name “carbonium ion” be henceforth reserved for pentacoordinated positive ions, and R_3C^+ cations be called “carbenium ions”. He also proposed the term “carbocation” to encompass both types and the IUPAC has accepted these definitions [6].

Among simple alkyl carbocations [7] the order of stability is tertiary > secondary > primary. There are many known examples of rearrangements of primary or secondary carbocations to tertiary, both in solution and in the gas phase.

The stability order can be explained by the polar effect and by hyperconjugation. In the polar effect, nonconjugated substituents exert an influence on stability through bonds (inductive effect) or through space (field effect). Since a tertiary carbocation has more carbon substituents on the positively charged carbon, relative to a primary one, there is a greater polar effect that leads to great stability. In the hyperconjugation explanation, we compare a primary carbocation with a tertiary one. It should be made clear that “the hyperconjugation concept arises solely from our model-building procedures. When we ask

whether hyperconjugation is important in a given situation, we are asking only whether the localized model is adequate for that situation at the particular level of precision we wish to use, or whether the model must be corrected by including some delocalization in order to get a good enough description” [8].

Mechanism of acid-catalyzed hydrocarbon reactions in superacid media and over solid zeolite

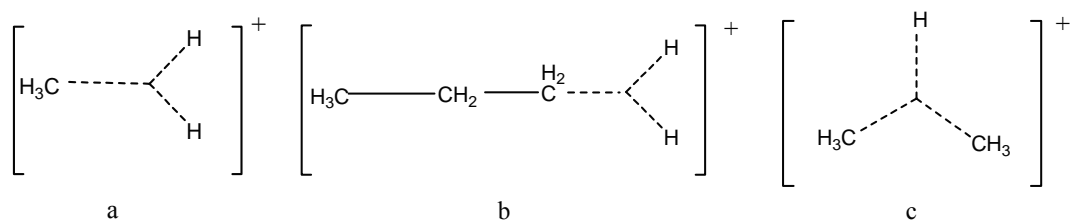
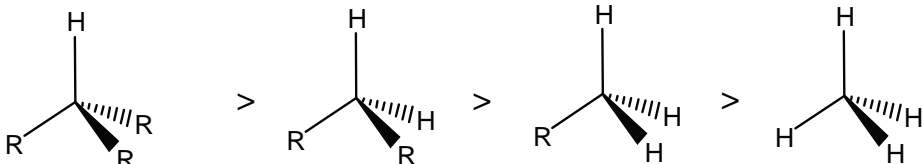
Protonation of saturated alkanes may result in the formation of non-classical pentacoordinated carbonium ions [9]. The high acidity of the catalysts and high temperature compensate for the well-known inertness of the starting material. It is widely accepted that the reactions proceed via an ionic mechanism [10]. The initial step is, however, often ascribed [11] as a proton attack on a C-C or a C-H bond, following the concept of σ -reactivity developed by Olah and his group [12].

The activation step of protolysis of a C-H or a C-C bond relies on the concept of σ -basicity (shown in Scheme 1) as proposed by Olah in 1972 [13] on the basis of the chemical reactions observed between alkanes and liquid superacids.

The simplest example is the methonium ion CH_5^+ which Olah has formulated as containing a three-centre, two-electron bond (Scheme 2a, indicated with dotted lines). Higher alkanes can be protonated both at C-H bonds (Scheme 2b) and at C-C bonds (Scheme 2c).

The activation of short-chain alkanes is one of the greatest challenges of the present catalysis research. Solid acid catalysts and more specifically acidic zeolites play an important role in the petroleum and chemical industries as highly active and selective catalysts [14-16]. The microporous structure of zeolites provides a large internal surface and selectivity effects related to diffusion and steric control on transition states. The development of experimental techniques for the *in situ* study of reactions on solids [17-18], has made possible the direct observation of the Brønsted acid sites and their interaction with adsorbed molecules.

According to Olah [9], the formation of hydrocarbon ions can be obtained in the gas phase



through the proton transfer between a cation precursor and its neutral species [19]. In other words, under normal conditions the proton transfer occurs by way of a generalized electrophilic reaction, in which it has been established that the hydrogen interacts with the saturated bond of the hydrocarbon [20].

The first interaction of saturated alkanes with the zeolite acid protons consists of a fast hydrogen exchange that can be monitored using isotopic labeling [21]. To explain the H/D exchange in propane and isobutane a mechanism based on classical trivalent carbenium ion intermediates has been proposed [22-24], while for methane and ethane [25, 26], in which only primary protons are available, the H/D exchange proceeds in a concerted step involving a carbonium ion with a pentacoordinated carbon atom. The existence of non-classical carbonium ions having a two-electron three-centre bond in the gas phase has been confirmed by mass spectroscopy [27, 28], and it has been observed that C-protonated species

are initially formed and they rearrange to H-protonated isomers which dissociate into hydrogen plus the corresponding carbenium ion [29, 30]. It is concluded that both carbenium and carbonium ions may exist as reaction intermediates only when the positive charge is not easily accessible to framework oxygen atoms. Otherwise, they will evolve so that the charge separation between the organic fragment and the zeolite framework is minimized, resulting in the formation of neutral species: adsorbed hydrocarbons or alkoxide complexes.

Carbonium ions in homogeneous phase

Carbonium ions are involved, as reaction intermediates or transition states, in the mechanism of many acid-catalyzed transformations of saturated hydrocarbons, and it is of interest to understand the mechanism of their formation, rearrangement and dissociation. The different structures for the methonium cation, CH_5^+ , were proposed theoretically and studied in great details [31-35].

The potential energy surfaces of isolated ethonium, C_2H_7^+ [36, 37], proponium, C_3H_9^+ [38], *n*-butonium, $n\text{-C}_4\text{H}_{11}^+$ [39] and iso-butionium, *i*- $\text{C}_4\text{H}_{11}^+$ [40] cations, as well as the protonation of alkanes by HF/SbF_5 superacids [41] were theoretically investigated using high level *ab initio* methods. These extensive studies showed that C-protonated alkanes are more stable than H-protonated ones, in agreement with the product distribution observed for the gas phase protonation of propane and isobutane, and also they explained the preferential protonation of the tertiary C-H bond of isobutane in liquid superacids. The geometries and relative energies of a large number of isomers of protonated *n*-alkanes (from C_4 to C_{20}) and their dissociation into ion-molecule complexes were systematically investigated at different levels of theory by East and coworkers [42]. They also found that both C-C and C-H protonated alkanes as well as weak complexes between alkanes and carbenium ions are intermediate species rather than transition states, and may exist on acid zeolites and in ionic liquids.

Since the role of five coordinated carbocations in the transformation of lower carbocations in higher cations, in the process of the transformation of methane into the highly desirable hydrocarbons and in other hydrocarbon transformations, it is of interest to understand the structural features of these species. In order to get a suitable improvement of the understanding of the chemical bonding in carbonium ions we employ the topological analysis of the electron density to investigate the general pattern of the electron density shared by the carbonium ions ($\text{C}=1\text{-}4$). This tool is based on the atoms in molecules (AIM) theory developed by Bader [43]. In order to facilitate the reading of this paper we introduce the basic concepts and terminology of the AIM theory.

The topological analysis of the electronic density

Bader's fundamental work in the sixties on molecular electron density distributions laid the foundations for the theory which was developed in the seventies and eighties by his research group, which became known as the theory of

Atoms in Molecules (AIM) [43]. In more recent literature this theory is often called the Quantum Theory of Atoms in Molecules (QTAIM) in recognition of its rigorous basis in quantum mechanics.

The theory relates the fundamental concepts of chemistry, such as chemical structure, chemical bonding, transferability of functional groups, and chemical reactivity, to the topology of the underlying electron-density distribution.

The topological properties of the electron distribution of a molecular or crystalline system are based on the gradient vector field of the electron density $\nabla\rho(\mathbf{r})$, and on the Laplacian of the electron density $\nabla^2\rho(\mathbf{r})$. The electron density distribution of the carbonium ions is described by $\rho(\mathbf{r})$, where \mathbf{r} is a vector in ordinary three-dimensional space and \mathbf{X} represents a particular set of the nuclear coordinates in space corresponding to the nuclear configurations of the carbonated structures. An atom in molecule is defined as region of real three-dimensional space bounded by a zero-flux surface. The points on this surface satisfy $\nabla\rho(\mathbf{r}) \cdot \mathbf{n}(\mathbf{r}) = 0$ where $\mathbf{n}(\mathbf{r})$ is the unit vector normal to this surface at \mathbf{r} . Two interacting atoms in a molecule form a critical point in the electron density, where $\nabla\rho(\mathbf{r}) = 0$, called a bond critical point (BCP) and it is abbreviated as \mathbf{r}_b . The pairs of gradient paths, which originate at a BCP and terminate at neighboring nuclei, define a line, through which the electron distribution, $\rho(\mathbf{r})$, is a maximum with respect to any lateral displacement. Linking two nuclei in a molecule with a nuclear equilibrium configuration, this kind of lines are called atomic interaction lines implying that two atoms are bonded to one another and in this instance this line is called a bond path. The network of bond paths for a molecule in a given nuclear configuration \mathbf{X} defines the molecular graph. Such a topological graph usually corresponds to the commonly drawn chemical bond network. The eigenvalues ($\lambda_1, \lambda_2, \lambda_3$) of the Hessian matrix of ρ_b , whose sum equals $\nabla^2\rho(\mathbf{r})$, indicate how rapidly the electron density changes on moving away from the BCP and represent the curvatures of the electron density along the principal axes of curvature. The CP's are labeled as (*r, s*) according

to their rank, r (number of non-zero eigenvalues), and signature, s (the algebraic sum of the signs of the eigenvalues).

Four types of CP's are of interest in molecules: (3, -3), (3, -1), (3, +1) and (3, +3). A (3, -3) point corresponds to a maximum in $\rho(\mathbf{r})$ and occurs generally at the nuclear positions. A (3, +3) point indicates electronic charge depletion and it is known as box critical point. (3, +1) points, or ring critical points, are merely saddle points. Finally, a (3, -1) point, or bond critical point, BCP, is generally found between two neighboring nuclei indicating the existence of a bond between them.

For a normal single bond, such as the C-C bond in ethane, the two negative curvatures (λ_1 and λ_2), which are perpendicular to the bond line, are equal. However, in the case of a double bond, one curvature (in the direction of the π bond) will be much smaller than the other two. The difference may be described by the ellipticity, ε , of the bond which is defined as $\varepsilon = (\lambda_1/\lambda_2) - 1$, where λ_2 is the curvature of smallest magnitude. For a single bond $\lambda_1 = \lambda_2$ and therefore $\varepsilon \approx 0$. For a double bond $|\lambda_1| > |\lambda_2|$ and therefore $\varepsilon > 0$. For the CC bond in an aromatic system, in general, ε is intermediate between a typical single and a typical double bond. For symmetrical triple bonds, since $\lambda_1 \approx \lambda_2$, ε is equal or close to zero. Large ε values indicate that the bond under study has an intrinsic instability and it will tend to undergo a distortion to relax to a stable form [44]. One can also determine the regions of space wherein the electron density is locally concentrated or depleted by inspecting the Laplacian of the electron density, $\nabla^2\rho(\mathbf{r})$. $\rho(\mathbf{r})$ is greater than the average of its values over an infinitesimal sphere centered on \mathbf{r} , where $\nabla^2\rho(\mathbf{r}) < 0$, and $\rho(\mathbf{r})$ is less than its average when $\nabla^2\rho(\mathbf{r}) > 0$.

Several properties that can be evaluated at a bond critical point, BCP from now on, constitute very powerful tools to classify the interactions between two fragments. Calculated properties at the BCP of the electronic density are labeled with the subscript "b" throughout this work.

When the negative eigenvalues dominate, the electronic charge is locally concentrated in the region of the BCP leading to an interaction

typically found in covalent or polarized bonds and being characterized by large ρ_b values, $\nabla^2\rho_b < 0$ and $|\lambda_1|/\lambda_3 > 1$. If the positive eigenvalue is dominant, on the other hand, the electronic density is locally concentrated at each atomic site. The interaction is now referred to as a closed-shell one and it is characteristic of highly ionic bonds, hydrogen bonds and van der Waals interactions. Its main features are relatively low ρ_b values, $\nabla^2\rho_b > 0$ and $|\lambda_1|/\lambda_3 < 1$.

Structural and topologic characterizations of carbonium ions (C=1-4)

Methonium ions

Although numerous experimental studies have been performed on the CH_5^+ ion [45-47] it was not until 1999 that Oka and collaborators succeeded in obtaining the high resolution IR spectrum of this chemical species [48]. Although it was not possible to carry out a detailed assignment of the individual lines due to the complexity of the obtained spectrum, the results seem to confirm theoretical predictions that this molecule is highly fluxional and that the term "structure" should have to be refined [28c, 31b, 49, 50].

The interest about the CH_5^+ cation led to numerous studies, mainly for the apparent difficulty in locating structures of minimum energy of well defined geometry, a fact that has not still been proven experimentally. Nevertheless, different structures for the methonium cation were proposed theoretically [33] (Figure 1). The energetic of these systems has been studied rigorously in the frame of the most sophisticated theory levels [31a, 31b, 32, 49a, 50-52].

High quality *ab initio* calculations [31a] have shown that the structure **1**, with C_s symmetry, is the most stable species and it corresponds to a minimum in the surface of potential energy. Therefore, it would be possible that these species could be observed experimentally. This result agrees with the fact that this cation can lose a hydrogen molecule.

The protonated methane possesses a surface of potential energy that involves about 120 identical

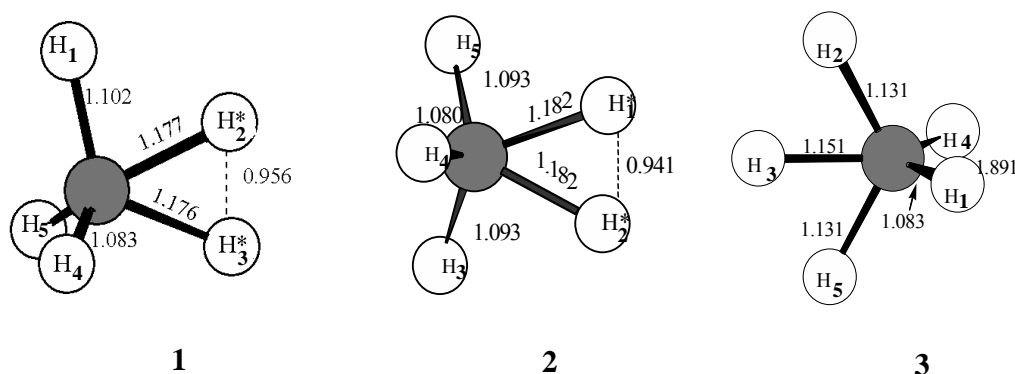


Figure 1. Optimized geometries of species of CH_5^+ ion calculated at MP2(full)/6-31G** level.

minima, each one involving a structure with a 3c-2e bond in the CH_2 group, and they can interconvert with a low amount of energy (with activation barriers of only about 0.1 to 0.8 kcal.mol^{-1}) [52].

Calculations have shown that, although the structure **1** (Figure 1) represents a true minimum of energy, the other structures (**2-3**) are practically isoenergetic to structure **1**. The calculated barrier of interconversion for **1-3** is of approximately 0.1 kcal.mol^{-1} . Schleyer and collaborators [31a] suggested that the CH_5^+ cation does not have a defined structure since the protons are extremely mobile and, therefore, the representation with a 3c-2e bond is an oversimplification.

Marx and Parrinello, using *ab initio* molecular dynamics calculations [53], concluded that the species CH_5^+ is better described by the structure with symmetry C_s (**1**), with a 3c-2e bond, as it had been suggested by Olah and collaborators in 1969, based on the fact that H_2 is formed by the reaction of methane with liquid superacid media, which supports a species where a H_2 moiety is complexed to a CH_3^+ cation, as in the species with C_s symmetry [12a]. In general, calculations show that the CH_5^+ cation undergoes extensive internal rearrangement (or, as Olah denominates, “bond-to-bond rearrangements”), and that the ion is best represented by the structure **1**.

In order to arrive at a comprehensive understanding of CH_5^+ , cutting-edge experimental and theoretical studies will be needed [53].

The topology of the electronic density charge was studied for CH_5^+ species [35] at *ab initio* level

using the Theory of Atoms in Molecules (AIM) developed by Bader [43].

The analysis of the charge density and the bond critical points (BCP) were applied in order to establish the features of the multicenter bonds in the different species **1**, **2** and **3** in CH_5^+ cation and to understand their high fluxionality. Two different topological situations could be defined: the species **1** and **2** present a 3c-2e (Figure 1a and 1b) but in the species **3** the absence of a 3c-2e bond is noteworthy (Figure 1c).

The topological properties at the BCPs of the C-H bonds in the CH_5^+ ion are characteristic of covalent bonds and they have large ρ_b (0.2895 a.u.) and $\nabla^2\rho_b$ (-1.1011 a.u.) values and $|\lambda_1/\lambda_3| > 1$.

The C-H* bonds of the cations **1** and **2** show lower ρ_b and less negative $\nabla^2\rho_b$ values (0.2198 a.u. and -0.5065 a.u., respectively), with topological properties characteristic of covalent type interactions. The high ellipticity values of the C-H* bonds indicate a structural instability [44b], probably associated to the existence of three-center-two-electrons bonds.

Figure 2a shows the contour map of the Laplacian distribution $\nabla^2\rho$ for the methonium cation, **1**, in the plane that contains the carbon atom and the two hydrogen atoms of the 3c-2e bond. The relatively small bond angle $\text{H}^*\text{-C-H}^*$ in CH_5^+ leads to a concentration of the electronic charge density involving the three atoms, giving place to a three center-two electrons bond $\text{H}^*\text{-C-H}^*$ type. It can be observed that the 3c-2e bond presents two critical points and its trajectories of bond are indicative of two C-H* bonds and the

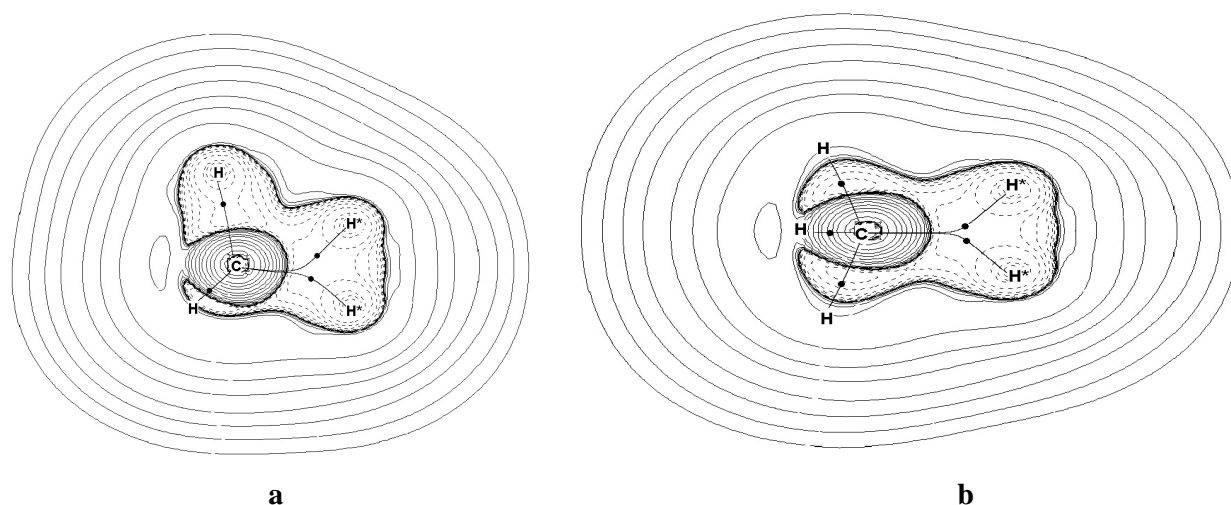


Figure 2. Laplacian of the electron density contour maps obtained with use of the PROAIM program [54] for: a) the methonium cation, 1, and b) the methonium cation, 2, in the plane that contains the 3c-2e bond. In both cases the molecular graphs are superimposed. Solid lines represent regions of electronic charge depletion, and dashed lines denote regions of electronic charge concentration. Bond critical points are indicated with circles. The contours of the Laplacian of the electronic density increase and decrease from a zero contour in steps of $\pm 2 \times 10^n$, $\pm 4 \times 10^n$, and $\pm 8 \times 10^n$, with n beginning at -3 and increasing by unity. The same set of contours and graphics features are used in all the figures of the present work.

missing of the trajectory binding both hydrogen atoms. Thus, at least from a topological point of view, the carbon atom in the CH_5^+ ion is really directly bound to five hydrogen atoms.

The contour map of the Laplacian, $\nabla^2\rho$, in specie **2** is shown in Figure 2b. Three center bond lies in the plane of the figure. It can be noted the absence of the bond path that connects both hydrogen atoms, in agreement with our previous explanation.

The topological distribution of the density of the structure **2** is quite similar to the specie **1**. Thus, the C-H* bonds that participate in the three center bond are energetically less stable than the other C-H bonds. However, in **2** the ellipticity values for these bonds increase significantly ($\epsilon = 4.04$ and 4.05 vs 2.05 and 2.67). This increment in the ellipticity value is correlated with an abrupt decrease in the perpendicular curvature λ_2 (-0.1637 and -0.1448 vs. -0.1008 and -0.1009).

The contour map of the Laplacian, $\nabla^2\rho$, in species **3** (C_{2v}) is shown in Figure 3. Several important differences regarding the previous two ones can be seen. Two fragments can be defined, CH_2 and CH_3 , but no 3c-2e bonds is observed. However, an

electron deficient region established against the C atom and the three H atoms that lie in the same plane can be described. This interaction called “four centers” defines a net of bond trajectories that present interesting topological properties: the three BCPs of the CH bonds show smaller ellipticity values (0.2230) than those found in the 3c-2e bonds of the remaining carbocationic species (2.0495 or 4.0464). The nuclei define a four center interaction where the electronic delocalization produced among the σ (C-H) bonds provide a stabilization of the three C-H bonds involved in this interaction (the remaining two C-H bonds are similar to those belonging to the non protonated species).

Ethonium ions

Experimental studies of gas-phase protonation [28c] showed the existence of isomeric C_2H_7^+ cations, with an energy difference of about 7-8 Kcal.mol^{-1} . These species were also characterized by UV spectroscopy in gas phase [49]. Carneiro *et al.* [36] performed ab initio calculations and they showed that the C-ethonium ion is more stable than H-ethonium cation by 4.4 Kcal.mol^{-1} . These results are consistent with H/D Exchange

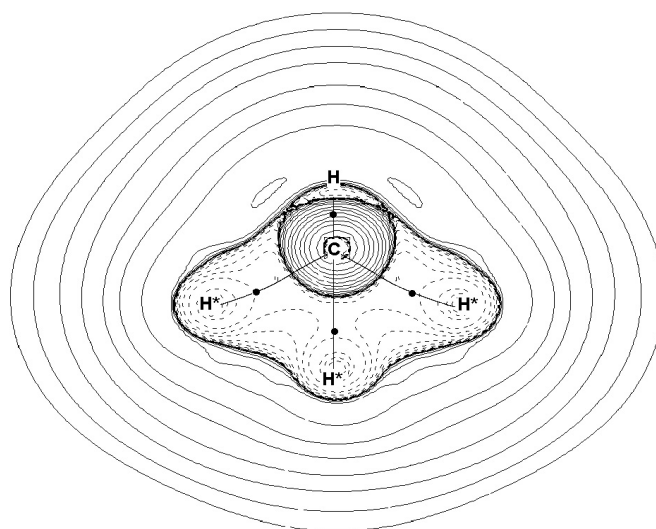


Figure 3. Laplacian of the electron density contour map and molecular graph obtained with use of the PROAIM program [54] for the methonium cation, **3**, in the plane that contains the four centers interaction.

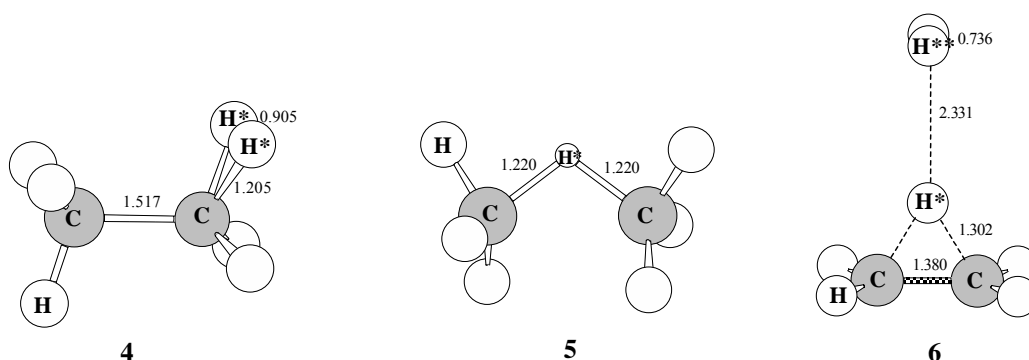


Figure 4. Optimized geometries of species of $C_2H_7^+$ ion calculated at MP2(full)/6-31G** level.

reactions in isotopically labeled superacids [55] and they are also in agreement with the formation of methane as a byproduct of the decomposition of ethane in superacid liquids.

Later on it have been shown [55] that $C_2H_7^+$ ion presents three isomers at low temperature: one isomer protonated on the σ_{C-C} bond, one protonated on the σ_{C-H} bond and another isomer resulting from the interaction of a H_2 molecule with the $C_2H_5^+$ ion. The van der Waals complex, $C_2H_5^+ \cdot H_2$, was significantly higher in energy and the C-ethonium ion was lower in energy.

Theoretical predictions of East *et al.* [56] have given the possibility of a reinterpretation of the

experimental results. Especially, experimental findings of Hiraoka y Kebarle [28c] and Yeh, Price and Lee [49b] reveals that the van der Waals complex may be better characterized as a solvated ion than as a H-ethonium isomer, as it was stated so far [28c, 36, 49b]. However, discrepancies between theoretical and experimental results are still significant so that further experiments are needed to clarify these differences.

Optimized geometries calculated at MP2(full)/6-31G** level of the cations H-ethonium, C-ethonium and the van der Waals complex $C_2H_5^+ \cdot H_2$ (structure **4-6**) are shown in Figure 4. The most relevant geometric parameters are also shown here.

No significant geometrics changes are observed by the proton insertion into the CC bond or when the proton is inserted in one of the CH bonds of ethane. On the contrary, in the $\text{C}_2\text{H}_5^+\cdot\text{H}_2$ cation the C-C bond distance is shorter than in ethane (1.380 Å against 1.522 Å, respectively).

The topology of the electronic density charge was studied for the C_2H_7^+ isomers [57] at *ab initio* level using the AIM theory [43].

The topological properties at the BCPs of the C-H bonds in H-ethonium ion (structure **4**) are characteristic of covalent bonds ($\rho_b = 0.2893$ a.u., $\nabla^2\rho_b = -1.0645$ a.u. and $|\lambda_1|/\lambda_3 = 1.7061$). It is interesting to note that in H-ethonium ion there is a BCP between two H atoms forming a C-H*-H* bond type and showing a different pattern to 3c-2e in CH_5^+ structure. The C-H* bond presents lower density values ($\rho_b = 0.2123$ a.u.) and less negative Laplacian of density values ($\nabla^2\rho_b = -0.3872$ a.u.) as well as in the H*-H* bond ($\rho_b = 0.2217$ a.u. and $\nabla^2\rho_b = -0.5989$ a.u., respectively), but also with topological properties characteristic of covalent type interactions. The high ellipticity values (2.4911 in C-H* bond and 1.7518 in H*-H* bond) are indicative of a structural instability, as it is found in three-center-two-electrons bonds. Figure **5a** shows the contour map of the Laplacian of

density distribution, $\nabla^2\rho$, for the H-ethonium ion, in the plane that contains the carbon atoms and 3c-2e bond. It can be observed that the 3c-2e bond presents two critical points: one BCP in C-H* bond and another BCP in H*-H* bond, both located at a region of charge accumulation.

In the C-ethonium ion (structure **5**) there is an H-bridge atom between the carbon atoms, forming a C-H*-C three center-two electron bond. There is not a critical point between the carbon atoms. The topological properties at the BCPs of the C-H* bonds are also characteristic of covalent bonds ($\rho_b = 0.1774$ a.u., $\nabla^2\rho_b = -0.3329$ a.u. and $|\lambda_1|/\lambda_3 = 1.5552$). Figure **5b** shows the contour map of the Laplacian of density distribution, $\nabla^2\rho$, for the C-ethonium ion, structure **5**, in the plane that contains the C-H*-C 3c-2e bond. This figure also shows the network of trajectory of the bond of the C-ethonium ion, where the BCPs are shown. It can be observed that the 3c-2e bond presents two critical points and that its trajectories of bond are indicative of one C-H* bond type.

In the van der Waals complex, structure **6**, the BCP at the C-C bond has high values of the electronic density and the Laplacian of the density ($\rho_b = 0.3227$ u.a. and $\nabla^2\rho = -1.0035$ u.a., respectively) and ellipticity value ($\varepsilon = 0.2519$) is

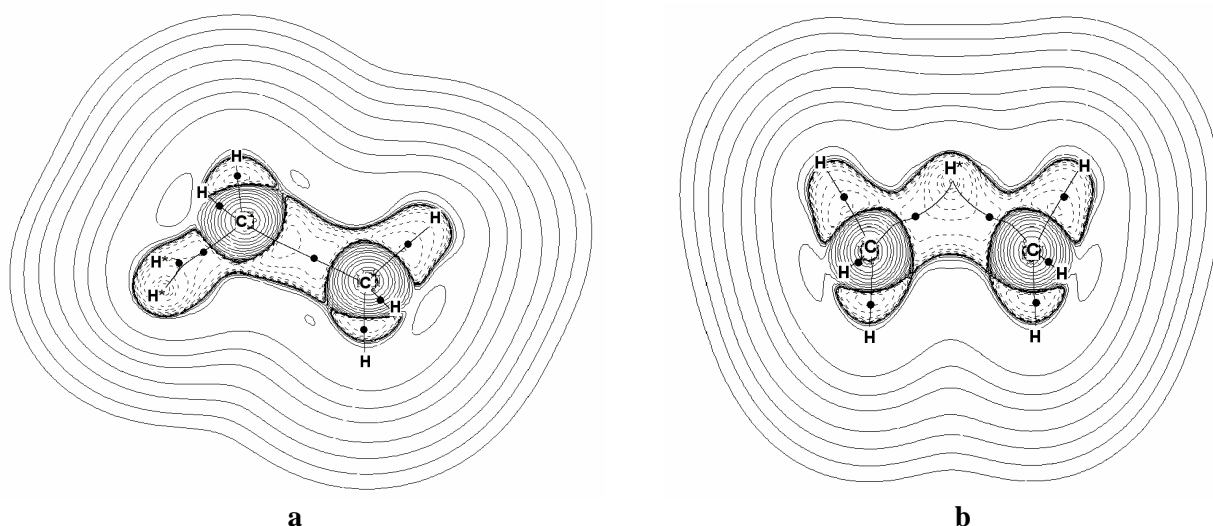


Figure 5. Laplacian of the electron density contour maps obtained with use of the PROAIM program [54] for: a) H-ethonium cation, 1, and b) C-ethonium cation, 2, in the plane that contains the 3c-2e bond. In both cases the molecular graphs are superimposed.

considerably higher than that found in the corresponding C-C bond in ethane ($\epsilon = 0.0000$), indicating that the density distribution has no axial symmetry ($\lambda_1 \neq \lambda_2$), as usually occurs in π bonds. It is interesting to note the large ellipticity exhibited by the C-H* bond ($\epsilon = 1.5676$). This fact suggests an intrinsic instability for those bonds and a tendency to relax to a more stable structure. The H-H bond of the hydrogen pseudomolecule has properties corresponding to a shared interaction ($\rho_b = 0.2660$ a.u.; $\nabla^2\rho_b = -1.1210$ a.u.) with a similar behavior to the H_2 isolated molecule ($\rho_b = 0.2744$ a.u. and $\nabla^2\rho_b = -1.4407$ u.a. at the same level of calculation). Finally, one BCP between the H* atom of the $C_2H_5^+$ moiety and the H** atoms is encountered. In this BCP electronic density values and the Laplacian of the density values are lower than others bonds, showing typical closed-shell features ($\rho_b = 0.0073$ u.a.; $\nabla^2\rho_b = 0.0209$ u.a. and $|\lambda_1|/\lambda_3 = 0.2006$), as it is characteristic of the van der Waals interactions. The ellipticity value is considerably higher ($\epsilon = 0.1003$) indicating a possible trend to decomposition of the complex in two fragments: $C_2H_5^+$ and H_2 .

Figure 6 shows the contour map of the Laplacian distribution for the complex $C_2H_5^+.H_2$ in the plane that contains the 3c-2e bond, C-H*-C. It can be observed that the 3c-2e bond is localized at a region of charge accumulation while the BCP between two moieties is located in a region of decrease of charge as previously anticipated by the topologic properties.

Proponium cations

Esteves *et al.* [38] had calculated the potential energy surface of the $C_3H_9^+$ cation, that results from the protonation of propane, at the MP4(SDTQ)/6-311++G**//MP2(full)/6-31G** level of calculation. They were capable to characterize six structures as minima on the potential energy surface. In addition to the four proponium cations, hypothetically formed by protonation in the primary C-H bond (7 and 8, Figure 7), secondary C-H bond (9, Figure 7) and C-C bond (10, Figure 7) of propane, two van der Waals complexes were also characterized as minima in the potential energy surface. Structure 11 (Figure 7) represents the complex formed

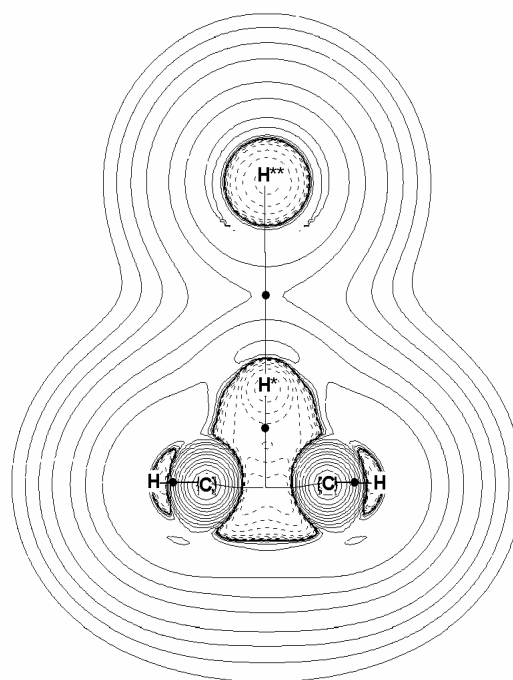


Figure 6. Laplacian of the electron density contour map obtained with use of the PROAIM program [54] for the van der Waals complex, structure 6, in the plane that contains the C-H*-C bond. Molecular graph is superimposed.

between the ethyl cation and methane and structure 12 (Figure 7) the complex formed between the isopropyl cation and hydrogen. At MP4/6-311++G**//MP2/6-31G** level, the C-proponium cation (10) was the lowest energy species with the van der Waals complex formed between the isopropyl cation and hydrogen (12) lying only $0.3 \text{ kcal.mol}^{-1}$ above. The H-proponium ions were significantly higher in energy. The 2-Hproponium was about 7 kcal.mol^{-1} and the 1-H-proponium about 10 kcal.mol^{-1} higher than structure 10. Structures 7 and 8 possess nearly the same energy.

The topology of the electronic density charge for $C_3H_9^+$ species, at an *ab initio* level using the AIM theory developed by Bader [43] was studied [58]. Calculations were carried out at the MP4SDTQ-(fc)/6-311+G**//MP2(full)/6-31G** level.

A 3c-2e bond of C-H*-H* type is found in all of the H-proponium cations and the topological distribution of the electronic charge density shows practically no differences. The electronic density

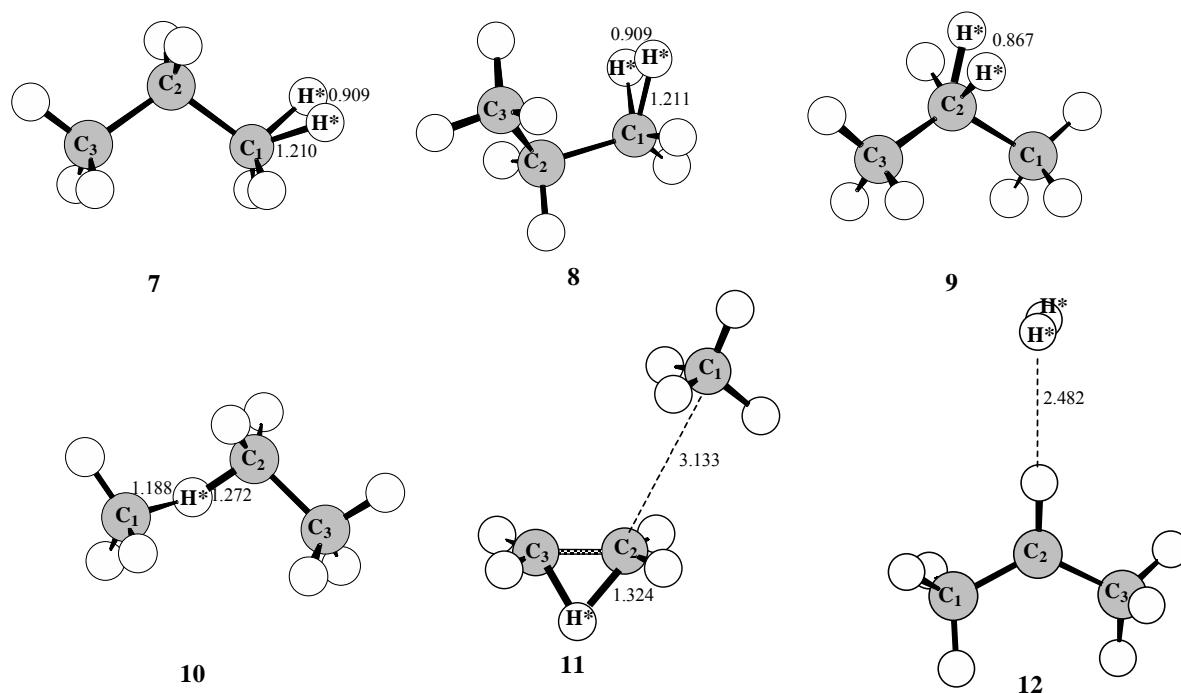


Figure 7. MP4(SDTQ)/6-311++G**/MP2(full)/6-31G** geometries of C_3H_9^+ isomers.

in the BCP of $\text{C}_1\text{-H}^*$, the primary H-carbonium ion, is rather higher ($\rho_b = 0.2125$ a.u. and 0.2123 a.u. in structures **7** and **8**, respectively) than the density in the $\text{C}_2\text{-H}^*$, a secondary H-carbonium ion ($\rho_b = 0.1946$ a.u.). The Laplacian of the density values show a decrease when the carbon atom changes from primary to secondary ($\nabla^2\rho_b = -0.4089$ a.u., -0.4081 a.u. and -0.2276 a.u., respectively). According to these values, it is possible to characterize the $\text{C}_{1,2}\text{-H}^*$ bonds as shared interactions. On the other hand, the electronic density and the Laplacian of the density values at $\text{H}^*\text{-H}^*$ bonds are increased ($\rho_b = 0.2198$ a.u., 0.2197 a.u. and 0.2267 a.u.; $\nabla^2\rho_b = 5849$ a.u., -0.5852 a.u. and -0.6844 a.u., respectively), because of the electronic distribution in the three center two-electron bonds.

Figure 8a shows the contour map of the Laplacian distribution, $\nabla^2\rho$, for the H-proponium ion, **7**. This figure allows one to distinguish the type of bonds, since the BCP at the shared interactions $\text{C}_1\text{-H}^*\text{-H}^*$ are located in a region of charge accumulation. It is interesting to note that there are two critical points in the 3c-2e bond and there

is only a BCP between C_1 and H^* ; and not any ring critical points were found.

The topological distribution of the electronic charge density on the C-proponium cation, **10**, shows significant differences with respect to the structures of the H-proponium cations. The electronic density at the two BCP of the C-H^* bonds of the three center bond $\text{C}_2\text{-H}^*\text{-C}_1$ are rather different. In fact, the density on the bond BCP of $\text{C}_1\text{-H}^*$ of the methyl group is higher than the density on the $\text{C}_2\text{-H}^*$ bond. These results are in agreement with the bond distances calculated for structure **4** (1.188 and 1.272 Å, respectively). In the $\text{C}_1\text{-H}^*$ bond $\nabla^2\rho_b < 0$ and $|\lambda_1|/\lambda_3 > 1$; ($\rho_b = 0.1893$ a.u. and $\nabla^2\rho_b = -0.4256$ a.u.) while in the $\text{C}_2\text{-H}^*$ bond $\nabla^2\rho_b < 0$ (-0.1725 a.u.) but $|\lambda_1|/\lambda_3$ is slightly lower than 1 (0.9525). These results indicate that while the $\text{C}_1\text{-H}^*$ bond corresponds to a shared interaction, the $\text{C}_2\text{-H}^*$ presents a different behavior that seems to be intermediate between a shared and a closed shell interaction. No ring critical point was found for the C-proponium cation.

Figure 8b shows the contour map of the Laplacian distribution, $\nabla^2\rho$, for the C-proponium ion, **10**, in

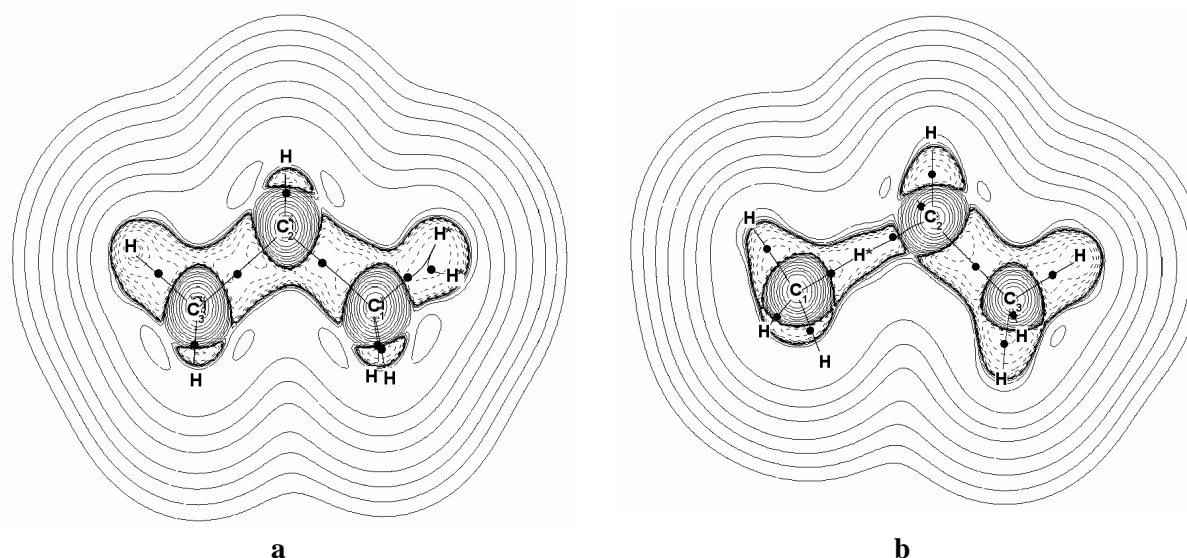


Figure 8. Laplacian of the electron density contour maps obtained with use of the PROAIM program [54] for the H-proponium ion, **7**, and C-proponium ion, **10**, in the plane that contains the 3c-2e bonds. The molecular graphs are superimposed.

the plane that contains the carbon atoms (the molecular graph is superimposed). It can be observed that the 3c-2e bond presents two BCPs though both of them are located in a region of charge accumulation.

Topological local properties at the BCPs of **11**, corresponding to the interaction between the ethyl cation and the methane molecule, show that although all bonds are of covalent nature, the C_1-C_2 (bond length 3.133 Å) exhibits the features of a closed shell interaction where ρ_b has a low value (0.0056 a.u.) and $\nabla^2\rho_b > 0$ (0.0245 a.u.). The ellipticity of this bond is high (2.5752) and since it is a measure of how far the density distribution is distorted from the axial symmetry of the bond this value would explain the higher energy of the complex.

The analysis of the more significant topological local properties at the BCP for structure **12**, corresponding to the interaction between the $s\text{-}C_3H_7^+$ cation and the hydrogen molecule, shows that the C-C bonds are typical covalent bonds. On the other hand, the values of the density charge and the Laplacian for the C_2-H^* bond show the characteristics of a closed shell interaction ($\rho_b = 0.0047$ a.u. and $\nabla^2\rho_b = 0.0156$ a.u.). The relationship $|\lambda_1|/\lambda_3 < 1$ (0.1841), as it generally happens in a van der Waals interaction.

The ellipticity for the C_2-H^* bond ($\varepsilon = 0.1411$) is greater than in the other C-H bonds ($\varepsilon = 0.0284$ for the C_1-H bond), indicating that this bond could be next to break [44]. The H^*-H^* bond has the topological properties of a shared interaction ($\rho_b = 0.2664$ a.u. and $\nabla^2\rho_b = -1.1238$ a.u.).

Figure 9 shows the contour map of the $\nabla^2\rho$ for the van der Waals complex, **12**, in the plane that contains the carbon atoms. It can be seen that the C_2-H^* bond critical point is located at a region of charge depletion, characteristic of a closed shell interaction. It can also be seen that the H^* atoms of the hydrogen molecule are not located on the plane defined by the carbon atoms, but in a plane almost perpendicular to it, in the direction of the C_2-H bond.

Butonium cations

n-Butionium cations

Esteves *et al.* [39] investigated the structure and energetics of the *n*-butionium cations ($n\text{-}C_4H_{11}^+$). The protonation of *n*-butane can take place at the primary C-H bonds (six overall), at the secondary C-H bonds (four overall), and at two distinct types of C-C bonds (two external and one internal) to form different isomeric structures of the $n\text{-}C_4H_{11}^+$ cation, as shown in Scheme 3.

The stability of the carbonium ions, formed by the protonation of the different σ bonds of *n*-butane, decreases in the order: 2-C-*n*-butonium > 1-C-*n*-butonium > 2-H-*n*-butonium > 1-H-*n*-butonium. The protonated butane species are isomeric to the

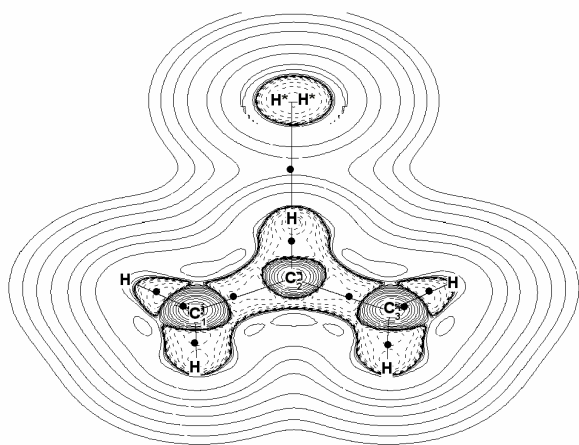
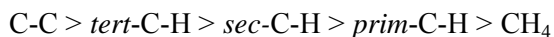


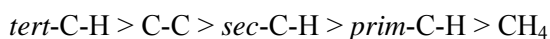
Figure 9. Laplacian of the electron density contour map obtained with use of the PROAIM program [54] for the van der Waals complex, **12**, in the plane that contains the carbon atoms. The molecular graph is superimposed.

isobutonium cations, which allow us to perform a direct energy comparison among the different $C_4H_{11}^+$ carbocations.

Esteves *et al.* [39], comparing the relative stability of the several $C_4H_{11}^+$ isomers, proposed the following σ -basicity scale:



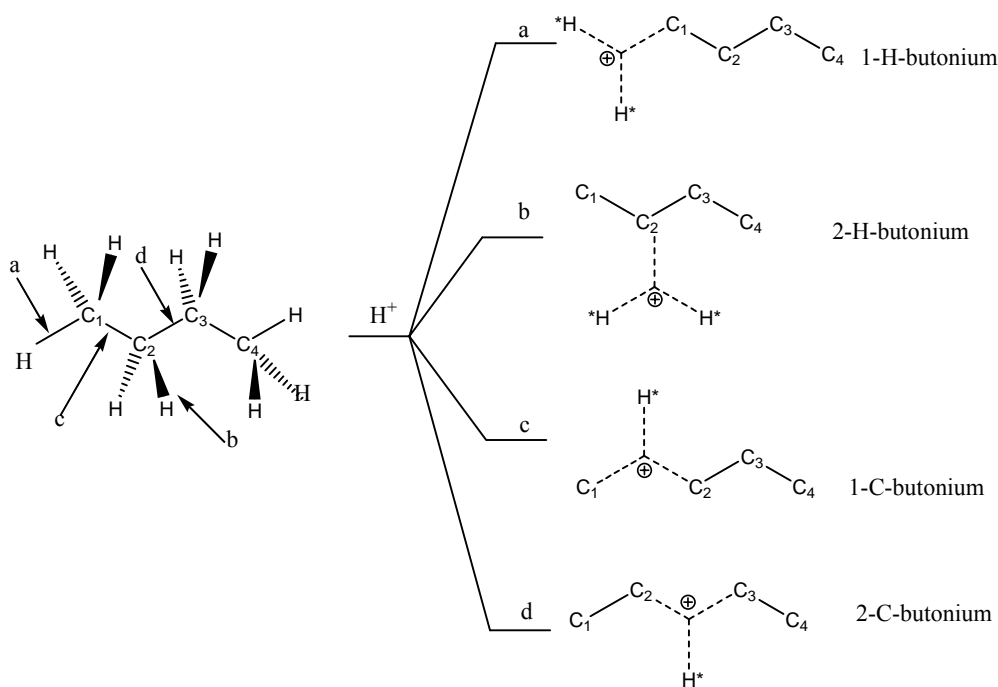
This scale differs slightly from the one proposed by Olah [13]:



since they do not correspond to the same phenomena. Olah's scale is related to the reactivity of the σ bond, which is a kinetic property, whereas Esteves' scale is based on relative stability, reflecting the basicity of the system. The later is related with thermodynamics of the protonation of the σ bonds.

Further studies [41a, 59] involving explicitly the anion and solvation of superacid models confirm the reactivity nature of Olah's scale [13].

The topology of the electronic density charge was studied [60] for *n*- $C_4H_{11}^+$ species, at *ab initio* level



Scheme 3. Nonequivalent bonds in *n*-butane leading to the different *n*-butonium ions by hypothetical protonation.

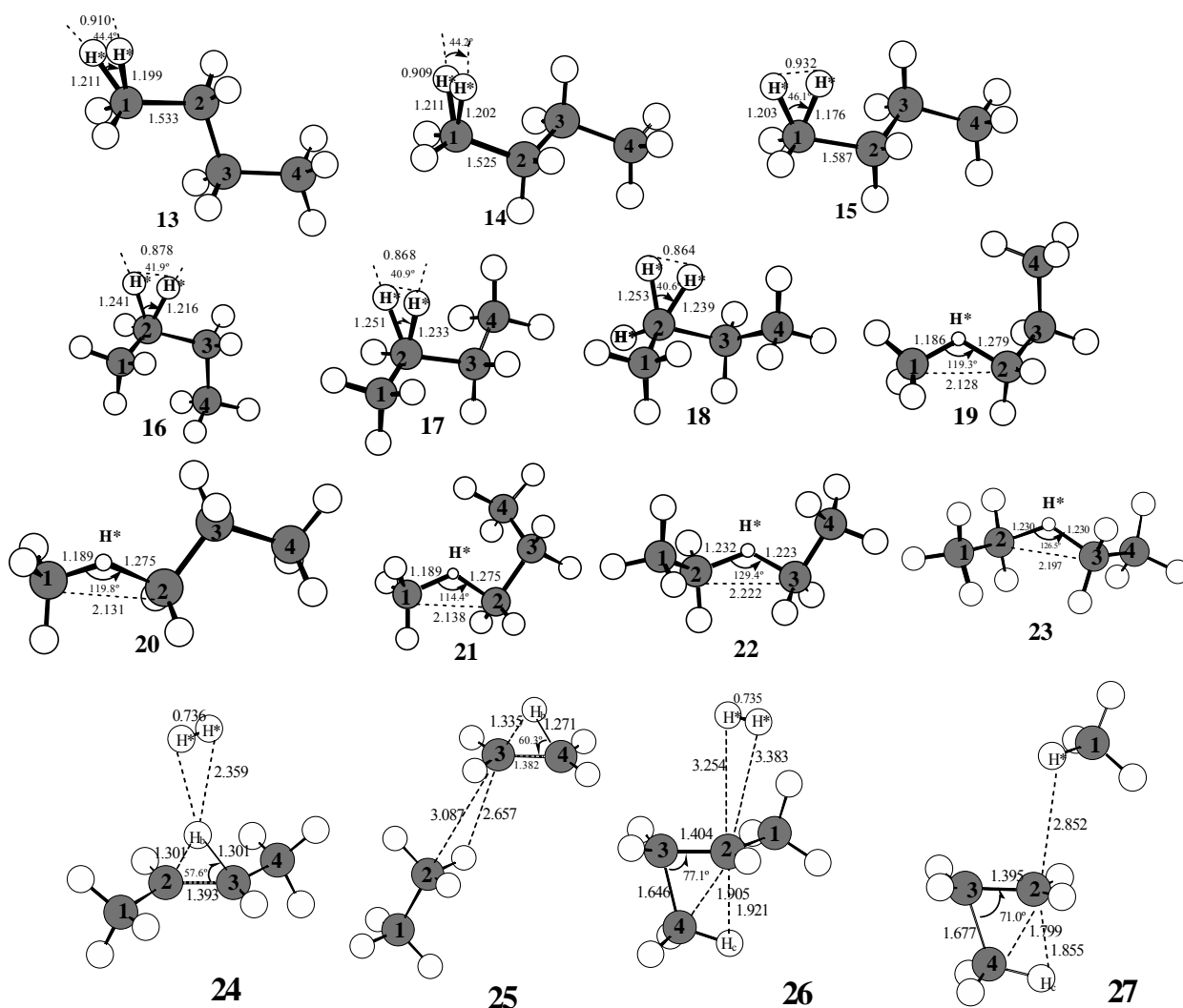


Figure 10. Geometries of $n\text{-C}_4\text{H}_{11}^+$ carbocations and van der Waals complexes at MP4SDTQ(fc)/6-311+G**/MP2(full)/6-31G** level.

using the AIM theory [43] in order to establish a relationship among the parameters that determine the stability order found for the different species and to relate them with the carbonium ions structure. Calculations were carried out at the MP4SDTQ-(fc)/6-311+G**/MP2(full)/6-31G** level.

Figure 10 shows the 15 structures that were located as minima in the potential energy surface. Protonation at the primary C-H bond produces structures **13-15** corresponding to conformational isomers of the 1-H- n -butonium cation. Protonation of the secondary C-H bonds leads to structures **16-18**, the conformer of the 2-H- n -

butonium cation. Protonation at primary C-C bonds (external) forms the conformers **19-21** corresponding to the 1-C- n -butonium ion, and protonation at the secondary C-C bond (internal) leads to the conformers **22-23** of the 2-C- n -butonium cation. Other minima in the PES were also found, and they correspond to van der Waals complexes. Structure **24** corresponds to the complex between the *sec*-butyl cation and H_2 . Structure **25** represents the C_2H_5^+ cation plus ethane. The complex between protonated methylcyclopropane plus hydrogen corresponds to structure **26** whereas protonated cyclopropane plus methane is shown as structures **27**. The

stability of the de van der Waals complexes decreased in the order **24** > **27** > **26** > **25** [39].

A 3c-2e bond of C-H*-H* type is found in all of the H-butyronium cations and there is a significant charge delocalization over the atoms in the 3c-2e region. The comparative analysis on the geometric and topological parameters at BCPs of the C-H* and H*-H* bonds in 1-H-*n*-butonium (structures **13-15**) and 2-H-*n*-butonium (**16-18**) cations allows one to achieve several conclusions. In the BCP at the C-H* bonds, the electronic density values and the Laplacian of the density values show a decrease when the carbon atom changes from primary to secondary ($\rho_b = 0.2200$ a.u. and 0.1994 a.u., and $\nabla^2\rho_b = -0.4744$ a.u. and -0.2407 a.u., respectively). Moreover, because of the electronic distribution in the three center two-electron bonds, the electronic density, ρ_b , and the Laplacian of the density, $\nabla^2\rho_b$, values at H*-H* bonds are increased ($\rho_b = 0.2195$ a.u. and 0.2257 a.u., and $\nabla^2\rho_b = -0.5816$ a.u. and -0.6604 a.u., respectively).

The C-carbonium ions show 3c-2e bonds with well defined topological characteristics. From an inspection of the **19-21** structures, corresponding to the 1-C_{*n*}-butonium ions, it can be seen that each one shows remarkable differences in the properties corresponding to the two C-H* bonds involved in the three center bonds. For example, in structure **19** the bond C₁-H* has $\rho_b = 0.1908$ a.u. and the bond C₂-H* has $\rho_b = 0.1413$ a.u. On the other hand, an inspection of 2-C-*n*-butonium cations, structures **22** and **23**, reveals that these structures have the highest symmetry among all structures and similar structural and topological characteristics. The two C_{sec}-H* bonds of the 3c-2e bonds as well as the neighbor C-C bonds have the same length and nearly similar topological properties (i.e. $\rho_b = 0.1630$ a.u. and $\rho_b = 0.1632$ a.u. in structure **23**), indicating that the charge of the cation is equally delocalized through the σ bonds of the carbon chain, which stabilizes the structure.

Figure 11 shows the contour map of the Laplacian distribution $\nabla^2\rho$ for the 2-C-*n*-butonium cation, structure **23**, in the plane that contains the 3c-2e bond. This figure allows one to see the shared interaction between C-H*-C atoms.

In complex **24**, the “H₂ molecule” is localized in a parallel plane from that formed by the carbon atoms, over a region of charge density accumulation between both secondary carbon atoms. The C₂-C₃ bond exhibits the characteristic of a covalent double bond ($\rho_b = 0.3172$ a.u.; $\nabla^2\rho_b = -0.9650$ a.u. and $\varepsilon = 0.2506$), whereas the other C-C bonds show a single covalent bond behavior (i.e. $\rho_b = 0.2662$ a.u.; $\nabla^2\rho_b = -0.7835$ a.u. and $\varepsilon = 0.0367$ in C₁-C₂ bond). A BCP is found among the hydrogen denoted as H_b (bridged) and the C₂ and C₃ atoms indicating the existence of a 3c-2e bond. The two hydrogen atoms, denoted as H*-H*, show the characteristic of a shared interaction between them ($\rho_b = 0.2661$ a.u. and $\nabla^2\rho_b = -1.1208$ a.u.), as in the isolated H₂ molecule. A single BCP is localized between both moieties showing the characteristic of a closed shell interaction ($\rho_b = 0.071$ a.u. and $\nabla^2\rho_b = 0.0204$ a.u.), as it generally happens in a van der Waals interaction. Finally, although the ellipticity value in the H₂ moiety is nearly zero ($\varepsilon = 0.0019$), a considerable ellipticity value is found for the interaction between both moieties ($\varepsilon = 0.1384$). This higher value is clearly indicative that this bond is near to be broken, and would explain the dissociation of the complex **24** into the *s*-butyl carbenium ion and the H₂ molecule.

Figure 12 shows the contour map of the Laplacian distribution $\nabla^2\rho$ for the complex **24** in the plane that contains the 3c-2e bond. It can be seen the BCP encountered between the bridge hydrogen (H_b) and the C₂ and C₃ atoms.

In structure **13**, the topological distribution of the electronic charge density in C-C bonds shows clearly differences in both fragments. In the C₂H₅⁺ cation, the C-C bond is involved in a 3c-2e bond, with the hydrogen atom bridged (H_b) with two carbon atoms in sp² hybridization fashion. This H_b is asymmetrically bonded to the carbon atoms because of the interaction with the ethane molecule. The topological properties are indicative of a double character bond in C-C ($\rho_b = 0.3220$ a.u.; $\nabla^2\rho_b = -1.0028$ a.u. and $\varepsilon = 0.2404$). On the other hand, the topological bond properties of the C₁-C₂ bond in the C₂H₆ moiety are similar to those corresponding to the ethane ($\rho_b = 0.2518$ a.u.; $\nabla^2\rho_b = -0.6754$ a.u. and $\varepsilon = 0.0000$).

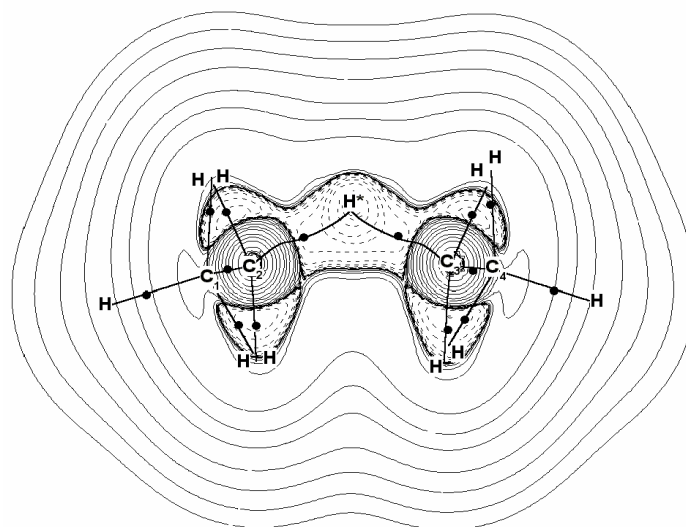


Figure 11. Laplacian of the electron density contour map obtained with use of the PROAIM program [54] for the structure **23** in the plane that contains the 3c-2e bond (C-H*-C). Molecular graph is superimposed.

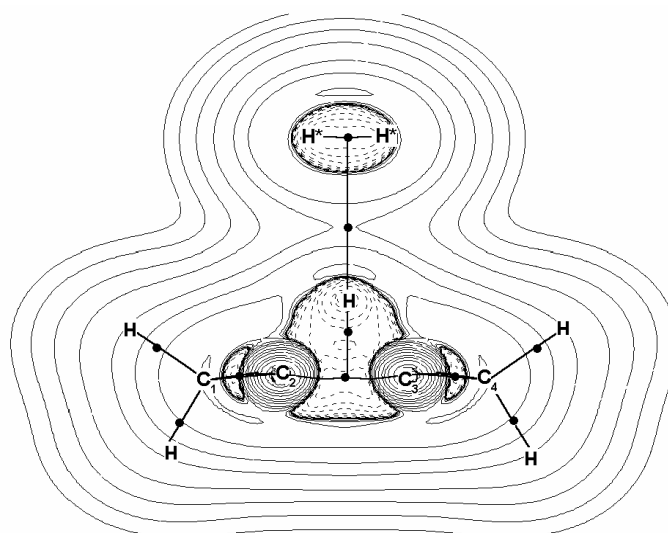


Figure 12. Laplacian of the electron density contour map obtained with use of the PROAIM program [54] for the van der Waals complex, structure **24**, in the plane that contains the 3c-2e bond.

The topology of the charge density in complex **26** shows only three BCPs between C-C bonds and no ring critical point is found as it would be expected because of their similarity with the methyl cyclopropane molecule. In addition, the properties at the H*-H* BCP ($\rho_b = 0.2667$ a.u.; $\nabla^2\rho_b = -1.1258$ a.u. and $\epsilon = 0.0005$) are indicative of a shared interaction with a similar behavior to

the H₂ isolated molecule. Contrary to expectation, structure **27** does not show a ring critical point. Thus, from the topological charge density point of view, structure **27** is more similar to a van der Waals complex between a primary 1-propyl cation and a CH₄ molecule than to a van der Waals complex between a protonated cyclopropane cation and a CH₄ molecule.

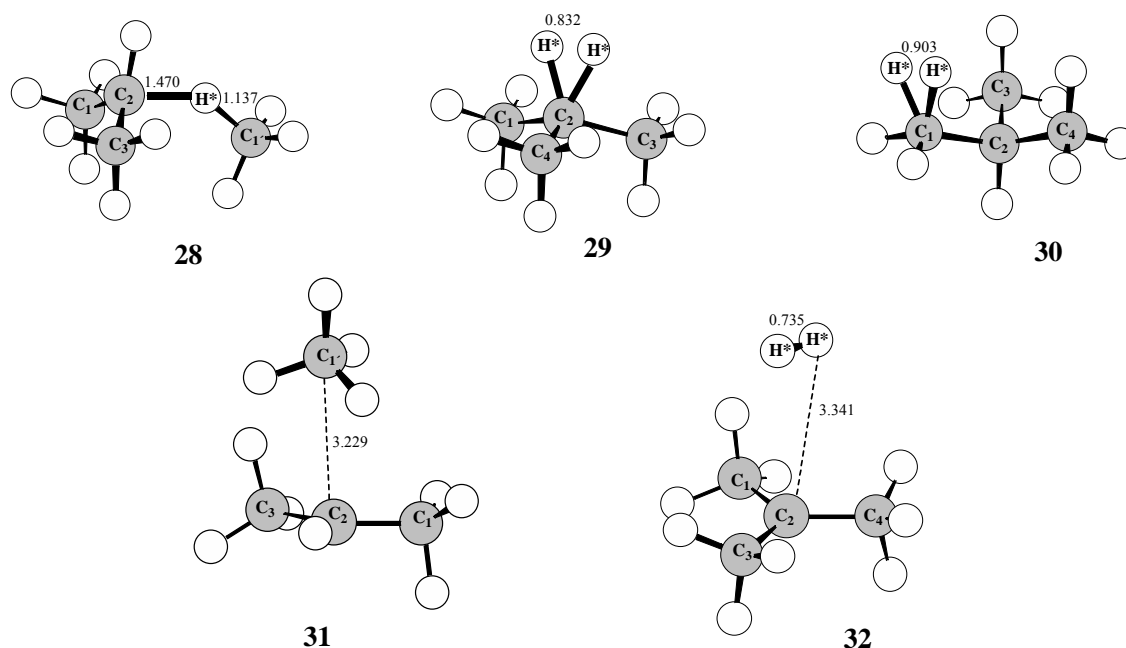


Figure 13. Geometries of $i\text{-C}_4\text{H}_{11}^+$ carbocations and van der Waals complexes at MP4(SDTQ)/6-311+G**/MP2(full)/6-31G** level.

iso-Butonium cations

At the *ab initio* level (calculations of Hartree-Fock, single-reference second-order Møller-Plesset perturbation theory (MP2) using the 6-31G** basis sets.), isobutonium cations show that five different stable structures could be characterized from the structural and energetic point of view [40a]. Among the isobutonium cations, the most stable structure corresponds to the C-isobutonium ion, structure **28** (Figure 13). The H-isobutonium cations, structures **29** and **30** (Figure 13), are significantly higher in energy. In **29**, the three-center bond involves $\text{C}_2\text{-H}^*\text{-H}^*$, where the C_2 corresponds to a tertiary carbon atom.

On the other hand, in **30**, the bond is formed among $\text{C}_1\text{-H}^*\text{-H}$, where C_1 is a primary carbon atom. The two energetically most favored structures correspond to van der Waals complexes: one between CH_4 and $i\text{-C}_3\text{H}_7^+$, structure **31** (Figure 13), and other, of lower energy, between H_2 and the $t\text{-C}_4\text{H}_9^+$ cation, structure **32** (Figure 13). At the MP4(SDTQ)/6-311++G**//MP2-(full)/6-31G** level, **32** is 4.26 kcal/mol lower in energy than **31** and about 5.5 kcal/mol more stable than **28** [40b]. The order of

stability among the isobutonium cations is in good agreement with the experimental results of isobutane protonation in the gas phase, where formation of methane and isopropyl cations is preferred, suggesting protonation in the C-C bond [61]. On the other hand, in liquid superacid, the main products are the *tert*-butyl carbenium ion and hydrogen, [1] in agreement with calculations of **32** being the most stable $i\text{-C}_4\text{H}_{11}^+$ species. The reasons for the greater stability of the C-isobutonium compared to the H-isobutonium are believed to be related to the charge distribution among the atoms and groups participating in the three-center bond. Hence, in **28**, the positive charge is better delocalized among the three atoms and it entails a lowering of the total energy.

The topology of the electronic density charge was studied [62] for all of the $i\text{-C}_4\text{H}_{11}^+$ species shown in Figure 13, at the *ab initio* level, using the theory of atoms in molecules (AIM) [43] (calculations were carried out using 6-311++G** basis sets).

A 3c-2e bond of $\text{C-H}^*\text{-H}^*$ type is found in both H-*i*-butonium cations, structures **29** and **30**. The comparative analysis on the topological parameters at BCPs of the C-H^* and $\text{H}^*\text{-H}^*$

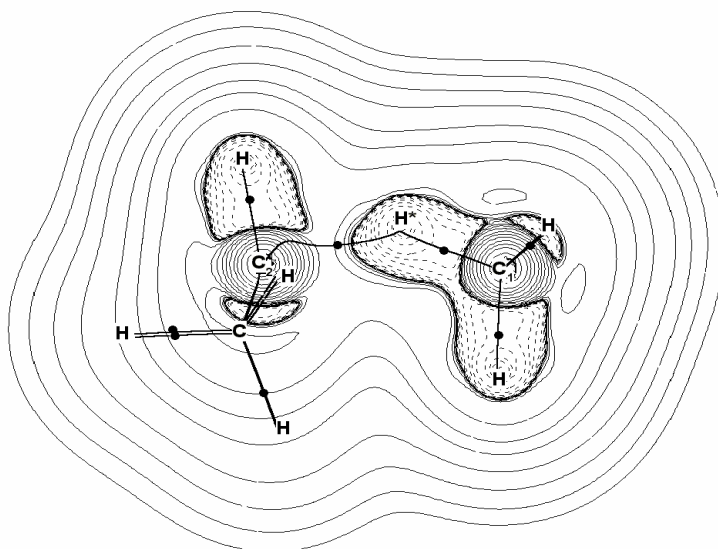


Figure 14. Laplacian of the electron density contour map obtained with use of the PROAIM program [54] for the C-isobutonium, structure **28**, in the plane that contains the 3c-2e bond, $C_1-H^*-C_2$. Molecular graph is superimposed.

bonds in structures **30** and **29** shows that in the BCPs at the C-H* bonds the electronic density values decrease when the carbon atom changes from primary to tertiary ($\rho_b = 0.2090$ a.u. and 0.1712 a.u., respectively). Moreover, because of the electronic distribution in the 3c-2e bonds, the ρ_b values at H*-H* bonds are increased (0.2200 a.u. and 0.2354 a.u., respectively).

The topological distribution of the electronic charge density on the C-isobutonium cation **28** shows significant differences with respect to the van der Waals complex, **31**. In the first one, the electronic density at the two BCPs of the C-H bonds found in the 3c-2e bond, $C_2-H^*-C_1$, is very different. In fact, the topological characteristics at BCPs allow us to characterize the C_1-H^* bond as a covalent bond ($\rho_b = 0.2250$ a.u. and $\nabla^2\rho_b = -0.4447$ a.u.) while the bond between C_2 and H^* corresponds to a closed shell interaction ($\rho_b = 0.0786$ a.u. and $\nabla^2\rho_b = 0.0654$ a.u.), as does that of the van de Waals interaction.

The contour map of the Laplacian distribution $\nabla^2\rho$ for the C-isobutonium ion **28**, in the plane that contains the $C_1-H^*-C_2$ bond (figure 14) allows one to differentiate both types of bonds because the critical point at the covalent bond C_1-H^* is located in a region of charge accumulation

whereas the critical point between C_2-H^* , corresponding to the van der Waals complex, is located in an area of charge depletion.

It was observed important changes in bond electronic distribution of **29** to give the van de Waals complex, **32**. In $t\text{-C}_4\text{H}_9^+$, the three primary carbon atoms resemble each other (C-C bond lengths are 1.459 Å, 1.459 Å and 1.457 Å). On the other hand, in **29**, one C-C bond, C_2-C_4 , is longer (1.541 Å) than the other two (1.520 Å). In **32**, the three bonds are shortened, and the density in the BCPs of the three C-C bonds increase compared to **29** ($\rho_b = 0.2885$ a.u.; 0.2885 a.u. and 0.2900 a.u. in **32** vs. ($\rho_b = 0.2354$ a.u.; 0.2560 a.u. and 0.2430 a.u. in **29**). This was explained by the hyperconjugation effect that takes place to stabilize the *tert*-butyl cation. The high ellipticity found for the C_2-H^* bond in **29** ($\epsilon = 2.4080$) suggests that this species will undergo a structural change [44b]. This is in agreement with the calculated potential energy surface of the $i\text{-C}_4\text{H}_{11}^+$ that shows that the interconversion of **29** in the van der Waals complex **32** occurs with negative activation energy. So, one must suppose that **29** spontaneously decomposes to **32** and, through this way, it cannot be formally considered as a discrete intermediate. The topological study of the charge

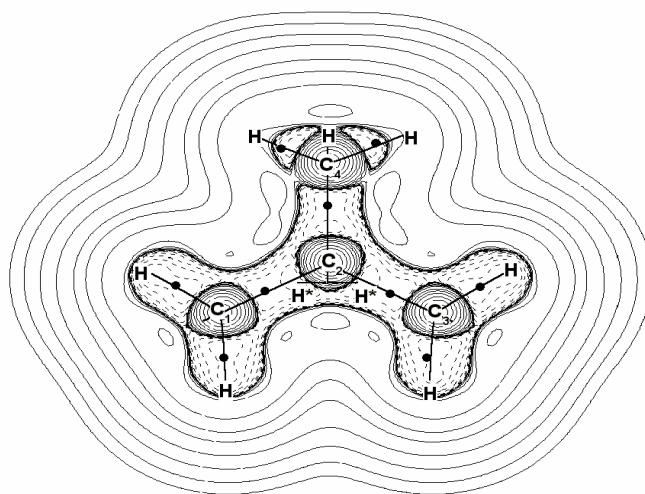


Figure 15. Laplacian of the electron density contour map obtained with use of the PROAIM program [54] of the van der Waals complex, structure **32**, in the plane that contains the four carbon atoms. The molecular graph is superimposed.

density reveals that an electronic delocalization takes place on the three C-C bonds in **32**. In this way, the van der Waals complex between the H_2 and the *tert*-butyl cation is stabilized, and it is the energetically most favored $i-C_4H_{11}^+$ structure. The Laplacian of the density distribution in the plane that contains the four carbon atoms of the planar *tert*-butyl cation shows (Figure 15) that each of the hydrogen atoms in the H_2 molecule is located symmetrically in an area where the Laplacian is negative, i.e., the concentration of the electronic charge density along the trajectory of the bond between C-C where the density is maximum.

Finally, it is interesting to note that in **31**, the complex between CH_4 and isopropyl cation, the van der Waals interaction takes place with the hydrogen atom of the methyl moiety that is far away 3.1740 Å from the isopropyl cation. On the other hand, there is no bond critical point with the methyl hydrogen atom that is separated with a distance of 2.889 Å. This seems to indicate that the most distant hydrogen atom presents a more favored stereo electronic arrangement.

CONCLUSIONS

Since the original and imaginative work of George A. Olah and co-workers in the early 1960s, a large number of carbocations have been prepared and their properties studied in greater

detail. Stable carbocations could be prepared through the use of extremely acidic compounds, far stronger than inorganic acids like sulphuric acid, hydrochloric acid, etc. These acids, generally known as superacids, are so strong that they can protonate such extremely weak bases as the alkanes. Thus, pentacoordinated carbonium ions have been obtained from methane higher alkanes and various cycloalkanes.

The study of those protonated species using spectroscopic techniques is accompanied with the employment of theoretical tools to complement the experimental efforts. In this review, we have presented an exhaustive structural and topologic study of methonium ethonium, protonium and butonium ions in order to get a suitable improvement of our understanding of the chemical bonding in these species.

The comparative analysis on the geometric and topological parameters of the carbonium ions (C=1-4) allow us to achieve the following conclusions:

1. The topology of the electronic density charge was studied for three species of the CH_5^+ cation at *ab initio* level of calculation and the BCPs were used in order to establish the features of the multicenter bonds in the different structures of the CH_5^+ cation and to understand their high fluxionality.

2. At MP2(full)/6-31G** level of calculation the $C_2H_7^+$ ion presents three isomers: one isomer protonated on the σ_{C-C} bond, C-ethonium, one protonated on the σ_{C-H} bond, H-ethonium, and another isomer resulting from the interaction of a H_2 molecule with the $C_2H_5^+$ ion. The van der Waals complex, $C_2H_5^+ \cdot H_2$, was significantly higher in energy and the C-ethonium ion was lower in energy.
3. Six different structures were studied for the $C_3H_9^+$ cation at the MP4(SDTQ)/6-311++G**//MP2(full)/6-31G** level of calculation: four proponium cations (two formed by protonation in the primary C-H bond, one formed by protonation in the secondary C-H bond and one formed by protonation of the C-C bond) and two van der Waals complexes. Among the proponium cations, the most stable structure corresponds to the C-proponium ion.
4. Fifteen different isomeric structures of the *n*-butonium cation ($n-C_4H_{11}^+$) were investigated at the MP4SDTQ-(fc)/6-311+G**//MP2(full)/6-31G** level of calculation. Protonation of *n*-butane at the primary C-H bond produces three structures corresponding to conformational isomers of the 1-H-*n*-butonium cation and protonation at the secondary C-H bonds leads to three 2-H-*n*-butonium cations. Protonation at primary C-C bonds forms three conformers corresponding to the 1-C-*n*-butonium ion and the protonation at the secondary C-C bond leads to two conformers of the 2-C-*n*-butonium cation. The stability of the carbonium ions, formed by the protonation of the different σ bonds of *n*-butane, decreases in the order: 2-C-*n*-butonium > 1-C-*n*-butonium > 2-H-*n*-butonium > 1-H-*n*-butonium. Other minima in the PES were also found and they correspond to four van der Waals complexes. The stability seems to be associated to higher stabilities of the carbon containing moieties (two primary carbenium ions in the case of the 2-C-*n*-butonium ion and a methyl and primary 1-propyl cation in the case of the 1-C-*n*-butonium cation).
5. At MP4(SDTQ)/6-311++G**//MP2-(full)/6-31G** level five different stable structures of isobutonium cations could be characterized. The two energetically most favored structures correspond to van der Waals complexes: one between CH_4 and $i-C_3H_7^+$ and other, of lower energy, between H_2 and the $t-C_4H_9^+$ cation. Then, the most stable structure corresponds to the C-isobutonium ion and the two H-isobutonium cations are significantly higher in energy. The order of stability among the isobutonium cations is in good agreement with the experimental results of isobutane protonation in the gas phase.
6. The 3c-2e bonds found in carbocationic species are established between two carbon atoms or carbon and hydrogen atoms, forming C-H-C and C-H-H bond types. So, a 3c-2e bond of C-H*-H* type is found in the H-alkylonium cations and a 3c-2e bond of C-H*-C type is found in the C-alkylonium cations. On the contrary, in CH_5^+ species the carbon atom is pentacoordinated and no BCP is found between any pairs of hydrogen atoms forming H*-C-H* bonds type. This situation is unique among the carbocations studied.
7. A novel four center-four electron bond was defined in one of the CH_5^+ isomers, where the positive charge can be delocalized between the four centers, displaying a singular contour map of the Laplacian of ρ in the plane containing these centers.
8. The topological analysis of the distribution of the charge density reveals that the stability of the protonated species depends fundamentally on the way in which the charge of the cation is delocalized around the 3c-2e bonds.
9. The stabilization degree of the H-carbonium species is related with an increase of the electronic density between the H* atoms and with a decrease of the density between H* and C atoms involved in the three centers bond. The stability of the species resulting of the C-H protonation increases as the properties of the H*-H* bond resemble that of the unperturbed H-H bond from the H_2 molecule, which points to a more stable carbenium ion interacting with the H_2 moiety.
10. The strong similarity between H-carbonium and C-carbonium cations lies in the redistribution of the electron density that accompanies their formation. In C-carbonium

cations the more stable species result when the delocalization of the electronic density on the atoms involved in the three centers bond and the remaining fragment are increased. Thus, the stability order is $C_{\text{tertiary}} > C_{\text{secondary}} > C_{\text{primary}}$.

REFERENCES

- Olah, G. A., Halpern, Y., Shen, J., and Mo, Y. K. 1973, *J. Am. Chem. Soc.*, 95, 4960.
- Olah, G. A. 1981, *Pure & Appl. Chem.*, 53, 201.
- Gomberg, M. 1902, *Ber. Dtsch. Che. Ges.*, 35, 2397.
- Smith, M. B. and March, J. 2007, *March's Advanced Organic Chemistry: Reactions, Mechanisms, and Structure*, Sixth Edition, Wiley, New Jersey.
- (a) Olah, G. A. 1971, *CHEMTECH*, 1, 566. (b) Olah, G. A. 1972, *J. Am. Chem. Soc.*, 94, 808.
- Gold, V., Loening, K. L., McNaught, A. D., and Sehmi, P. 1987, *Compendium of Chemical Terminology: IUPAC Recommendations*, Blackwell Scientific Publications, Oxford.
- Olah, G. A. and Olah, J. A. 1969, In: Olah, G. A. and Schleyer, P. v. R. *Carbonium Ions*, Vol. 2, Wiley & Sons, New York.
- Lowry, T. H. and Richardson, K. S. 1987, *Mechanism and Theory in Organic Chemistry*, 3rd ed., HarperCollins, New York.
- Olah, G. A., Prakash, G. K. S., and Sommer, J. 1985, *Superacids*, Wiley-Interscience, New York.
- Corma, A. 1995, *Chem. Rev.*, 95, 559.
- (a) Corma, A., Miguel, P. J., and Orchilles, V. A. 1994, *J. Catal.*, 145, 171. (b) Corma, A., Planelles, J., Sandoz-Marin, J., and Thomas, F. 1985, *J. Catal.*, 93, 30. (c) Haag, W. O. and Dessau, R. M. 1984, In: *Proceedings 8th International Congress in Catalysis; DECHEMA* Frankfurt am Main, Berlin, Vol. 2.
- (a) Olah, G. A., Klopman, G., and Schlosberg, R. H. 1969, *J. Am. Chem. Soc.*, 91, 3261. (b) Olah, G. A., and Olah, J. A. 1971, *J. Am. Chem. Soc.*, 93, 1256. (c) Olah, G. A., Mo, Y. K., and Olah, J. A. 1973, *J. Am. Chem. Soc.*, 95, 4939.
- Olah, G. A. 1973, *Angew. Chem. Int. Ed. Eng.*, 12, 173.
- Pines, H. 1981, *The Chemistry of Catalytic Hydrocarbon Conversion*, Academic Press, New York.
- Jacobs, P. A. 1977, *Carboniogenic Activity of Zeolites*, Elsevier, New York.
- (a) Corma, A. 2003, *J. Catal.* 216, 298. (b) Corma, A. 1995, *Chem. Rev.*, 95, 559. (c) Corma, A., Fornés, V., and Ortega, E. 1995, *J. Catal.*, 92, 284.
- Haw, J. F., Nicholas, J. B., Xu, T., Beck, L. W., and Ferguson, D. B. 1996, *Acc. Chem. Res.*, 29, 259.
- Farneth, W. E. and Gorte, R. J. 1995, *Chem. Rev.*, 95, 615.
- Williams, J. E., Buss, V., and Allen, L. C. 1971, *J. Am. Chem. Soc.*, 93, 6867.
- Olah, G. A. and Lukas, J. 1967, *J. Am. Chem. Soc.*, 89, 2227.
- Narbeshuber, T. F., Stockenhuber, M., Brait, A., Seshan, K., and Lercher, J. A. 1996, *J. Catal.*, 160, 183.
- Sommer, J., Habermacher, D., Jost, R., Sassi, A., Stepanov, A. G., Luzgin, M. V., Freude, D., Ernst, H., and Martens, J. 1999, *J. Catal.*, 181, 256.
- Hua, W., Sassi, A., Goeppert, A., Taulelle, F., Lorentz, C., and Sommer, J. 2001, *J. Catal.*, 204, 460.
- Schoofs, B., Schuermans, J., and Schoonheydt, R. A. 2000, *Micropor. Mesopor. Mater.*, 99, 35.
- Hua, W., Goeppert, A., and Sommer, J. 2001, *J. Catal.*, 197, 406.
- Schoofs, B., Martens, J. A., Jacobs, P. A., and Schoonheydt, R. A. 1999, *J. Catal.*, 183, 355.
- (a) Field, F. H. and Munson, M. S. B. 1965, *J. Am. Chem. Soc.*, 87, 3329. (b) Field, F. H., Franklin, J. L., and Munson, M. S. B. 1963, *J. Am. Chem. Soc.*, 85, 3575. (c) Wexler, S. and Hesse, N. 1962, *J. Am. Chem. Soc.*, 84, 3425.
- (a) Hiraoka, K. and Kebarle, P. 1975, *Can. J. Chem.*, 53, 970. (b) Hiraoka, K. and Kebarle, P. 1975, *J. Chem. Phys.*, 63, 394. (c) Hiraoka, K., Kebarle, P. 1976, *J. Am. Chem. Soc.*, 98, 6119.
- Hiraoka, K. and Kebarle, P. 1980, *Can. J. Chem.*, 58, 2262.
- Blair, A. S., Heslin, E. J., and Harrison, A. G. 1972, *J. Am. Chem. Soc.*, 94, 2935.

-
31. (a) Schleyer, P. v. R. and Carneiro, J. W. M. 1992, *Comput. Chem.*, 13, 997. (b) Schreiner, P. R., Kim, S. J., Schaefer, H. F., and Schleyer, P. V. R. 1993, *Chem. Phys.*, 99, 3716.
32. Marx, D. and Parrinello, M. 1995, *Nature*, 375, 216.
33. Collins, S. J. and O' Malley, P. J. 1996, *J. Chem. Soc., Faraday Trans.*, 92(22), 4347.
34. Olah, G. A. and Rasul, G. 1997, *Acc. Chem. Res.*, 30, 245-250.
35. Okulik, N. B., Peruchena, N. M., and Jubert, A. H. 2006, *Phys. Chem. A*, 110, 9974.
36. Carneiro, J. W. M., Schleyer, P. V. R., Saunders, M., Remington, R., Schaefer, H. F. III., Rauk, A., and Sorensen, T. S. 1994, *J. Am. Chem. Soc.*, 116, 3483.
37. Carneiro, J. W. D., Schleyer, P. V., Saunders, M., Remington, R., Schaefer, H. F., Rauk, A., and Sorensen, T. S. 1999, *J. Am. Chem. Soc.*, 121, 7345.
38. Esteves, P. M., Mota, C. J. A., Ramírez-Solís, A., and Hernández-Lamonedá, R. 1998, *J. Am. Chem. Soc.*, 120, 3213.
39. Esteves, P. M., Alberto, G. G. P., Ramírez-Solís, A., and Mota, C. J. A. 2000, *J. Phys. Chem. A*, 104, 6233.
40. (a) Mota, C. J. A., Esteves, P. M., Ramírez-Solís, A., and Hernández-Lamonedá, R. 1997, *J. Am. Chem. Soc.*, 119, 5193. (b) Esteves, P. M., Mota, C. J. A., Ramírez-Solís, A., and Hernández-Lamonedá, R. 1998, *Top. Catal.*, 6, 163.
41. (a) Esteves, P. M., Ramírez-Solís, A., and Mota, C. J. A. 2001, *J. Phys. Chem. B*, 105, 4331. (b) Esteves, P. M., Alberto, G. G. P., Ramírez-Solís, A., and Mota, C. J. A. 1999, *J. Am. Chem. Soc.*, 121, 7345.
42. (a) Hunter, K. C. and East, A. L. L. 2002, *J. Phys. Chem. A*, 106, 1346. (b) Seitz, C. and East, A. L. L. 2002, *J. Phys. Chem. A*, 106, 11653. (c) Li, Q. B., Hunter, K. C., Seitz, C., and East, A. L. L. 2003, *J. Chem. Phys.*, 119, 7148. (d) Hunter, K. C.; Seitz, C.; East, A. L. L. 2003, *J. Phys. Chem. A*, 107, 159.
43. Bader, R. F. W. 1990, *Atoms in Molecules. A Quantum Theory*, Oxford Science Publications, Clarendon Press, London.
44. (a) Kohler, H. J. and Lischka, H. H. 1978, *Chem. Phys. Lett.*, 58, 175. (b) Cremer, D., Kraka, E., Snee, T. S., Bader, R. F. W., Lau, C. D. H., Nguyen-Dang, T. T., and MacDougall, P. J. 1983, *J. Am. Chem. Soc.*, 105, 5069.
45. (a) Boo, D. W. and Lee, Y. T. 1993, *Chem. Phys. Lett.*, 211, 358. (b) Boo, D. W., Liu, Z. F., Suits, A. G., and Lee, Y. T. 1995, *Science*, 269, 57.
46. (a) Hiraoka, K. and Kebarle, P. 1975, *J. Am. Chem. Soc.*, 97, 4179. (b) Hiraoka, K. and Mori, T. 1989, *Chem. Phys. Lett.*, 161, 111. (c) Hiraoka, K., Kudaka, I., and Yamabe, S. 1991, *Chem. Phys. Lett.*, 184, 271.
47. (a) Heck, A. J. R., de Koning, L. J., and Nibbering, N. M. M. 1991, *J. Am. Soc. Mass Spectrom.*, 2, 453. (b) Oka, T. 1988, *Philos. Trans. R. Soc. London Ser. A*, 324, 81.
48. White, E. T., Tang, J., Oka, T. 1999, *Science*, 284, 135.
49. (a) Müller, H., Kutzelnigg, W., Noga, J., Klopper, W. 1997, *J. Chem. Phys.*, 106, 1863. (b) Yeh, L. I., Price, J. M., and Lee, Y. T. 1989, *J. Am. Chem. Soc.*, 111, 5597.
50. Schreiner, P. R. 2000, *Angew. Chem. Int. Ed.*, 39, 3239.
51. Collins, S. J. and O' Malley, P. 1994, *J. Chem. Phys. Lett.*, 228, 246.
52. Kolbuszewski, M. and Bunker, P. R. 1996, *J. Chem. Phys.*, 105, 3469.
53. Marx, D. and Parrinello, M. 1999, *Science*, 284, 59.
54. Klieger-König, W., Bader, R. F. W., and Tag, T. H. 1982, *J. Comp. Chem.*, 3, 317.
55. Sommer, J., Bakula, J., Hachoumy, M., and Jost, R. 1997, *J. Am. Chem. Soc.*, 119, 3274.
56. East, A. L. L., Liu, Z. F., Mc Cague, C., Cheng, K., and Tse, J. S. 1998, *J. Phys. Chem. A*, 108, 10903.
57. Unpublished results.
58. Okulik, N., Peruchena, N., Esteves, P., Mota, C., and Jubert, A. 2000, *J. Phys. Chem. A*, 104, 7586.
59. Esteves, P. M., Ramírez-Solís, A., and Mota, C. J. A. 2000, *J. Braz. Chem. Soc.*, 11, 345 (available at <http://www.s bq.org.br/jbcs/>).
60. Okulik, N. B.; Sosa, L. G.; Esteves, P. M.; Mota, C. J. A.; Jubert, A. H.; Peruchena, N. M. 2002, *J. Phys. Chem. A*, 106, 1584.
61. Aquilanti, V., Galli, A., Guidoni, A. G., and Volpi, G. G. 1968, *J. Chem. Phys.*, 48, 4310.
62. Okulik, N., Peruchena, N. M., Esteves, P. M., Mota, C. J. A., and Jubert, A. 1999, *J. Phys. Chem. A*, 103, 8491.